International Journal of New Horizons in Physics

http://dx.doi.org/10.18576/ijnhp/040102

Effect of Dilute Zn Doping on the Optical Properties of CdTe Thin Films

E. Márquez[1], M. Abdel-Rahman[2] and E. R. Shaaban[3,]*

[1]Departamento de Fisica de la Materia Condensada, Facultad de Ciencias, Universidad de Cádiz, 11510 Puerto Real (Cádiz), Spain.
[2]Department of Physics, Faculty of Science, El-Minia University, El-Minia, Egypt.
[3]Department of Physics, Faculty of Science, Al-Azahar University, Assiut, 71542, Egypt.

Received: 21 Oct. 2016, Revised: 22 Nov. 2016, Accepted: 24 Dec. 2016.
Published online: 1 Jan. 2017.

Abstract: The present study reports the synthesis of polycrystalline $Zn_xCd_{(1-x)}Te$ (x = 0,0.025, 0.050,0.075 and 0.100) using the chemical reaction in terms of ball milling. Ternary $Zn_xCd_{(1-x)}Te$ thin films were grown onto glass substrates at the temperature of 373 K using thermal evaporation technique. X-ray diffraction study showed that films are polycrystalline with cubic phase, which are preferentially oriented along the (111) direction. The refractive indices have been evaluated in transparent region using the envelope method, which has been suggested by Swanepoel. The optical energy gap were calculated in the strong absorption region of transmittance and reflectance spectrum. It was observed that the refractive index, *n*, deccreases but the energy gap increases with increasing the the dilute Zn, at expense of Cd, in $Zn_xCd_{(1-x)}Te$ thin films.

Keywords: $Zn_xCd_{(1-x)}Te$; EDAX; XRD; Refractive index; Optical Band Gap.

1. Introduction

Binary chalcogenide alloys such as ZnTe, CdSe and CdTe have semiconducting properties, which are well suitable for the fabrication of solar energy in photo electrochemical or photo voltaic devices [1-4]. Ternary $Zn_xCd_{(1-x)}Te$ alloys, which can be synthesised using the combination of ZnTe and CdTe or Cd, Te and Zn have important applications in the field of optoelectronic devices, visible-region-light emitting devices, light-detecting devices, photovoltaic conversion (solar cells), X-ray and γ-ray detection [2, 5-8]. Many techniques were used for preparation $Zn_xCd_{(1-x)}Te$ thin films such as chemical deposition, vacuum evaporation using two source [9], physical vapour transport [10] and molecular beam epitaxy [10, 11]. Due to a lack of reports on the possibility of obtaining the variable band gap films of ZnCdTe using the diffusion process. This is one of the important semiconductor compounds, as a top device in a high efficiency tandem solar cell structure, due to its tunable physical parameter [12]. Therefore, the aim of this paper is to fully understand the behavior of the optical constants, refractive index, n and extinction, k furthermore energy gap as a function of composition.

2. Experimental Details

Different composition of ternary polycrystalline $Zn_xCd_{(1-x)}Te$ alloys (with x = 0, 0.025, 0.05, 0.075 and 0.10)) were taken in molecular stoichiometric proportional weight of high purity (99.999% produced by Aldrich) analytical grade of ZnTe and CdTe powders according to the following

relation:

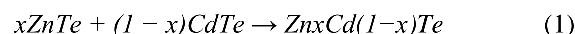

$$xZnTe + (1 - x)CdTe \rightarrow ZnxCd(1-x)Te \qquad (1)$$

At room temperature, the powders were mixed together in a mechanical ball mortar for about 1 hour. After that, the mixed powders were then pressed into a circular disk shape pellet. Such pellets were used as the starting materials from which the thin film will be prepared. The different sets of samples of varying compositions of $Zn_xCd_{(1-x)}Te$ were deposited via evaporation of the compound in vacuum higher than 10^{-6} Pa under controlled growth conditions of various compositions onto the precleaned glass substrates at the temperature of 373 K), using a conventional coating unit (Edward 306A).

The rate of evaporation thickness of the film thickness was controlled using a quartz crystal DTM 100 monitor. The deposition rate was maintained 10 Å/s constant throughout the sample preparations. The structure of the prepared samples were studied by XRD analysis (Philips X-ray diffractometry (1710)) with Ni-filtered Cu Kα radiation with λ = 0.15418 nm). The intensity data were collected using the step scanning mode with a small interval (2θ = 0.05°) with a period of 10 s at each fixed value to yield

*Corresponding author e-mail: esam_ramadan2008@yahoo.com

© 2017 NSP
Natural Sciences Publishing Cor.

reasonable number of counts at each peak maximum. The compositional analysis of the obtained films was done by energy dispersive X-ray spectrometer (EDXS) unit interfaced to scanning electron microscope (SEM) (Philips XL) operating at an accelerating voltage of 30 kV. The relative error of determining the indicated elements does not exceed 2.9%.

X-ray energy dispersive spectroscopy (EDAX) spectrum obtained for $Zn_{0.1}Cd_{0.9}Te$ sample are shown in Fig. 1. The representative Cd and Te peaks are clearly seen in the spectrum and no traces of other elements were noticed in the spectra confirming the purity of the samples. It is also notable that the elemental analysis results are consistent with the dopant concentration employed for the preparation of the samples. The transmsmission and reflections measurements were carried out using a double-beam(Shimadzu UV-2101 combined with PC) computer-controlled spectrophotometer, at normal incidence of light and in a wavelength range between 300 and 2500 nm.

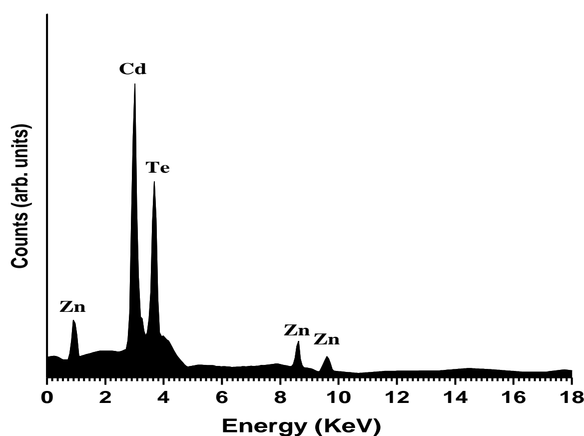

Fig. 1: EDAX spectrum checked for $Zn_{0.1}Cd_{0.9}Te$ film

3. Results and Discussion

3.1 X-Ray Diffraction of Thin Films

The X-ray diffraction pattern of vacuum evaporated $Zn_xCd_{(1-x)}Te$ thin films is shown in Fig. 2. The diffraction characteristic peaks for the cubic structure of CdTe (zincblende) are observed at $2\theta = 23.85^o$, 39.3^o and 46.5^o corresponding to the (111), (220), and (311) planes, respectively [13]. The sharp diffraction line indicates a good crystalline quality with the (111) preferred crystalline orientation of all the films. In general, in all evaporated films, the (111) direction is the preferred orientation of the CdTe crystallites. $Zn_xCd_{(1-x)}Te$ thin films have a spectral shift toward higher diffraction angles, due to the substitution of Zn atoms for Cd atoms in the CdTe matrix.

The shifting of peak positions of these prominent diffraction lines suggests the formation of solid solution corresponding to $Zn_xCd_{(1-x)}Te$ material from the basic starting compounds CdTe and ZnTe. Fig. 1 shows that the maximum intensity diffraction peaks {(111) and (220)} shift significantly from the usual position and the full-width at half maximum (FWHM) values also varies while we increase the Zn^{2+} concentration in CdTe. This can be explained based on the smaller atomic radius of Zn (1.35 Å) as compared to Cd (1.51 Å) [14], and the fact that incorporation of Zn^{2+} into CdTe crystal lattice may introduce some lattice distortion.

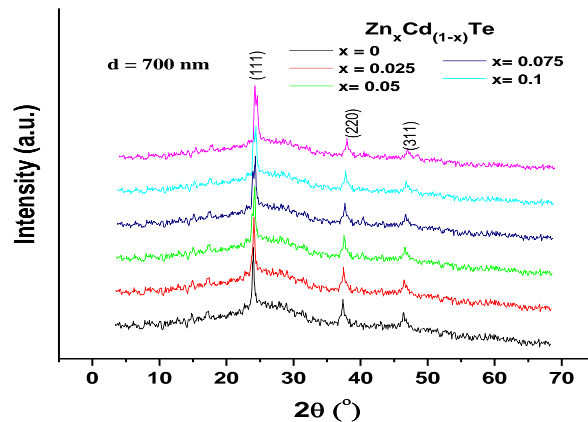

Fig. 2: XRD patterns of $Zn_xCd_{(1-x)}Te$ films at thickness equal 700 nm.

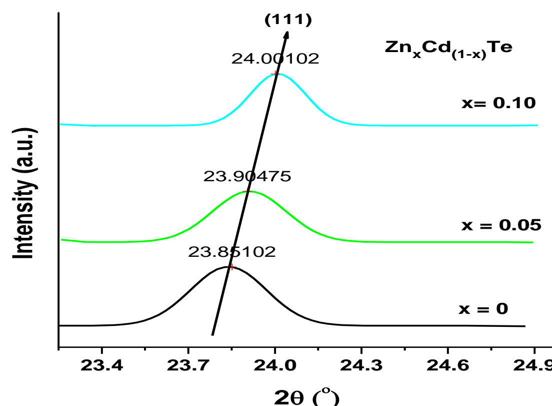

Fig. 3: Pattern shift of (111) peaks toward higher diffraction angles of $Zn_xCd_{(1-x)}Te$ films

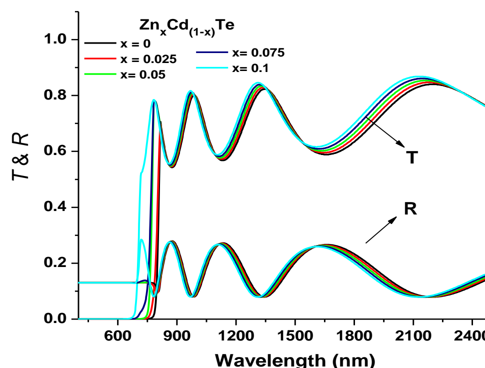

Fig. 4: The variations of transmission and reflection

© 2017 NSP
Natural Sciences Publishing Cor.

spectra versus wavelength for the $Zn_xCd_{(1-x)}Te$ deposited thin films at thickness = 700 nm.

3.2. Optical Properties

Fig. 4 shows the variations of transmission and reflection spectra with wavelength for the $Zn_xCd_{(1-x)}Te$ deposited thin films. It can be seen that the non-shrunking interference fringes (fringes of equal chromatic order FECO) observed in transmission spectra at longer wavelength (300-2500 nm) indicate the homogeneity and smoothness of the deposited films.

3.2.1. Determination of the Refractive Index

The film thickness, d, and refractive index, *n,* as the function of wavelength λ, are calculated from the optical transmittance spectrum of the as-deposited films in terms of *Swanepoel* method [15-17]. This method is dependent the idea of creating the envelopes of contractive interference maxima and destructive interference minima. Fig. 5 shows the spectral distribution of *T*(λ) and *R*(λ) for the *CdTe* thin film of thickness equal to 700 ± 1% nm, as an example of those under study. In this figure, the interference occurs due to multiple reflections of the incident beam inside the film, which results in an oscillating curve. This oscillation also confirm that the prepared film is proven to be uniform. Therefore, it is necessary to draw the envelopes curves for maxima and minima, which illustrated in Fig. 5 by the different symbol of the two curves. These envelopes are very carefully drawn using computer program (origin version 7). This method is based on determination of the corresponding tangent points between the set of oscillatory data and the envelopes.

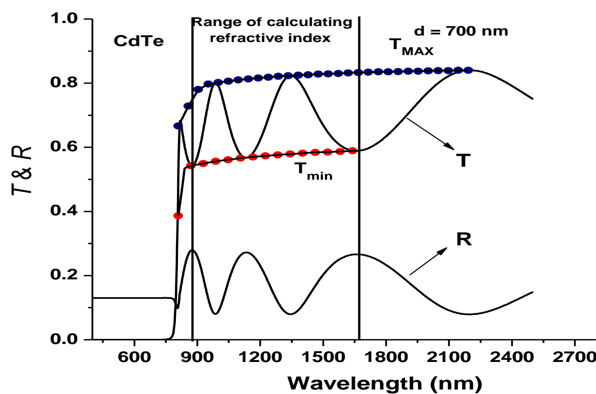

Fig. 5: The spectral distribution of *T* and *R* for the *CdTe* thin film of thickness equal to 700 nm. T_{Max} and T_{min} according to the text.

The main steps for the calculation of envelopes are: (*i*) data smoothing fit (*ii*) estimation of the location of the upper and lower tangential points and finally (*iii*) using of the third-order of exponential decay for interpolation through the estimated upper and lower tangential points. A distinct advantage of using the envelopes of the transmission spectrum rather than only the transmission spectrum is that, the envelopes are slow-changing functions of λ, whereas the transmission spectrum varies rapidly with λ. Once the tangential points at λ_i, between the two envelopes and the transmission spectrum are known, the refractive index can be calculated.

The approximate value of the refractive index of the film *n* at any wavelength in the spectral region of medium and weak absorption given by the equation [15]

$$n = \left[N + (N^2 - s^2)^{\frac{1}{2}} \right]^{\frac{1}{2}} \tag{2}$$

Where

$$N = 2s \frac{T_M - T_m}{T_M T_m} + \frac{s^2 + 1}{2}$$

Here T_M and T_m are the values of transmittance of lower and higher envelope curve of the T-λ plots. On the other hand, the values of the refractive index of the substrate are obtained from the transmission spectrum of the substrate, T_s using the well-known equation as follows [18]:

$$s = \frac{1}{T_s} + (\frac{1}{T_s} - 1)^{\frac{1}{2}} \tag{3}$$

The film thickness can be calculated using the refractive indices of two adjacent maxima (or minima) at λ_1 and λ_2 using the following expression

$$d = \frac{\lambda_1 \lambda_2}{2(\lambda_1 n_2 - \lambda_2 n_1)} \tag{4}$$

Fig. 6 illustrates the dependence of refractive index *n* as a function of wavelength for $Zn_xCd_{(1-x)}Te$ deposited thin films with thickness equal 700 ± 1% nm. It is obvious that, refractive index of each composition has the tendency to increase towards lower wavelength values (higher frequencies) which is consistent with normal dispersion. At higher wavelength values (lower frequencies), the refractive index tends to a constant or static value for each composition i.e. the films become non-dispersive at high wavelengths.

3.2.2. Determination of the absorption coefficient and the optical band gap

For the strong absorption region, the absorption coefficient α of different composition of $Zn_xCd_{(1-x)}Te$ thin films, the variation of the absorption coefficient obeys the relation [19]:

$$\alpha = \frac{1}{d} \ln \left[\frac{(1-R)^2 + \left[(1-R)^4 + 4R^2T^2 \right]^{1/2}}{2T} \right] \tag{5}$$

where *d* is the sample thickness.

© 2017 NSP
Natural Sciences Publishing Cor.

The obtained values of α for $Zn_xCd_{(1-x)}Te$ thin films at thickness equal 700 ± 1% nm as a function of photon energy, *hv*, are illustrated in Fig. 7. The inset shows the region of calculating optical band gap.

It is known that pure semiconducting compounds have a sharp absorption edge (corresponding to forbidden energy bandgap) [20-23]. Fig. 7 shows the dependence of the absorption coefficient, α, on photon energy *(hν)* for polycrystalline $Zn_xCd_{(1-x)}Te$ thin films. In Fig. 7, it is clearly observed that the spectral distribution of the absorption coefficient decreases with increasing the Zn content as expense of Cd in $Zn_xCd_{(1-x)}Te$ thin films. Knowing the values of absorption coefficient *α* of the films under study, the extinction coefficient k can be calculated using the relation

$$\mathrm{k} = \frac{\alpha\lambda}{4\pi} \quad (6)$$

The dependence of extinction coefficient κ of the studied $Zn_xCd_{(1-x)}Te$ thin films on the wavelength λ is shown in Fig. 8. It is obvious that, k for each composition has the tendency to increase towards lower wavelengths corresponding to strong electronic absorption between valence and conduction band and tends to zero at longer wavelengths

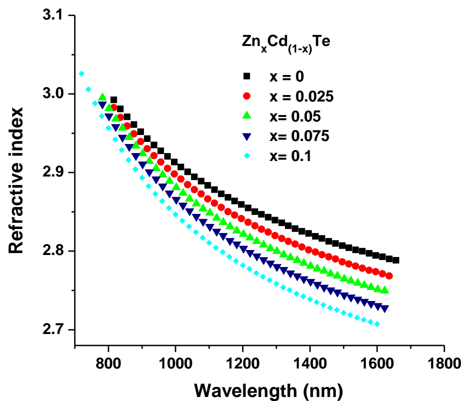

Fig. 6: The dependence of refractive index *n* as a function of wavelength for $Zn_xCd_{(1-x)}Te$ deposited thin films with thickness equal to 700 ± 1% nm.

where the absorption coefficient is nearly zero. Values of the optical energy gap E_g^{opt} of the films under investigation are determined for $\alpha \geq 10^4$ cm^{-1}, in the range where the optical absorption is due to extended state transitions. Since, E_g^{opt} is a measure of the energy gap between valence and conduction band edges. The absorption data extracted from transmittance spectrum are analyzed using the classical relation for near edge optical absorption of semiconductors given as [24, 25]

$$\alpha(h\upsilon) = \frac{K(h\upsilon - E_g^{opt})^r}{h\upsilon} \quad (7)$$

where *A* is a constant, *r* is a constant equal to 1/2, 2, 1/3 or 2/3 for indirect allowed, direct allowed, indirect forbidden and direct forbidden transition, respectively [25]. The best fit for $Zn_xCd_{(1-x)}Te$ thin films is found to follow the variation of $(\alpha h\nu)^2$ vs. *hν* as observed in Fig. 9 which confirms direct allowed band gap transition in $Zn_xCd_{(1-x)}Te$ thin films.

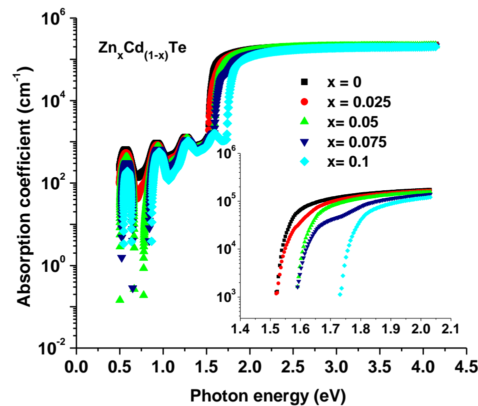

Fig. 7: Absorption coefficient for $Zn_xCd_{(1-x)}Te$ thin films with thickness equal to 700 ± 1% nm as a function of photon energy *hv*. The inset shows the region of calculating optical band gap.

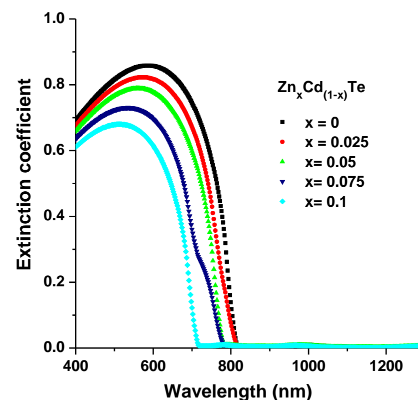

Fig. 8: Extinction coefficient of the $Zn_xCd_{(1-x)}Te$ thin films as a function of wavelength with thickness equal with 700 ± 1% nm

© 2017 NSP
Natural Sciences Publishing Cor.

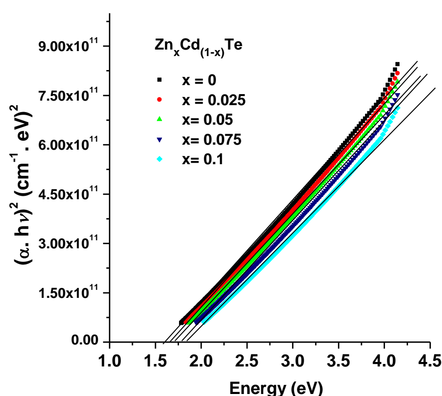

Fig. 9: The variation of $(\alpha h\nu)^2$ vs. $h\nu$ of the $Zn_xCd_{(1-x)}Te$ thin films with thickness equal to 700 ± 1% nm.

The optical gap can be obtained by extrapolating the straight line portion of the plot $(\alpha h\nu)^2$ versus $h\nu$ to zero absorption coefficient as shown in Fig. 9. Fig. 10 displays the change of optical energy gap, E_g^{opt} as a function of Zinc concentration in the $Zn_xCd_{(1-x)}Te$ thin films. The quadratic expression for the dependence of E_g^{opt} with Zn content (x) based in the virtual crystal approximation theory is Y =1.54543+3.24571 X- 6.85714 X^2. In this case E_g^{opt} when $x = 0$ is the E_g^{opt} of CdTe. The value of E_g^{opt} of CdTe calculated in this work is in a good agreement with that reported in previous work [7, 26].

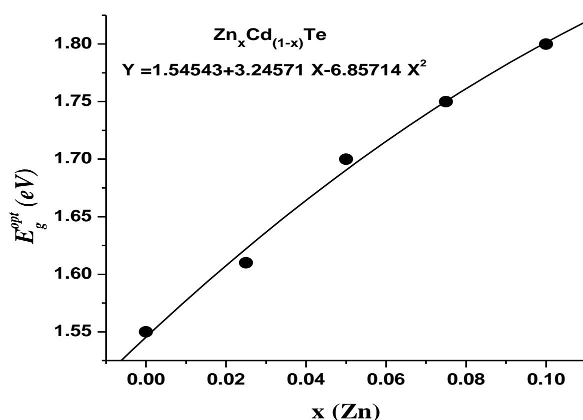

Fig. 10: Band gap energy as a function of the Zn concentration in the $Zn_xCd_{(1-x)}Te$ films.

4. Conclusions

In conclusion, polycrystalline thin films of CdTe doped with Zn^{2+} ions with different doping concentrations (x = 0, 0.025, 0.05, 0.075 and 0.10) were prepared by the thermal evaporation technique. XRD studies confirms and the prepared films are in the cubic phase and ED AX analysis revealed that the composition of different elements present in the films is consistent with added-amount of dopant in preparation step. The optical characterization shows that the refractive index of the polycrystalline $Zn_xCd_{(1-x)}Te$ thin films decreases and the fundamental band gap increases with increasing Zn content. The E_g^{opt} of Zn doped CdTe nano-crystals blue shifted with the increases of dopant concentration. The control of optical properties of CdTe by adding dilute Zn^{2+} ions have an important applications in the field of optoelectronic devices and photovoltaic conversion (solar cells).

References

[1] K. R. Murali, A.C. Dhanemozhi and R. John, J. Alloys & Comp. 464 (2008), p. 383.

[2] K. C. Bhahada, B. Tripathi, N. K. Acharya, P. K. .Kulriya and Y. K. Vijay, Applied Surface Science 255 (2008), p. 2143.

[3] F. Chowdhury, Journal of Electron Devices 10 (2011) 448.

[4] E. R. Shaaban, Ishu Kansal, S. H. Mohamed and J. M. F. Ferreira, Physica B: Condensed matter 404 (2009) 3571.

[5] Y. Yang, W. Zhang and Mater. Lett. 58 (2004) 3836.

[6] P. Roy, J. R. Ota and S. K. Srivastava, Thin Solid Films 515 (2006) 1912.

[7] E.R. Shaaban, N. Afify and A. El-Taher, J. Alloys & Comp. 482 (2009), p. 400.

[8] I. T. Sinaoui, F. Chaffar Akkar, F. Aousgi and M. Kanzari, Int. J. Thin Fil. Sci. Tec. 3, No. 1 (2014) 19.

[9] R. Weil, M. Joucla, J. L. Loison, M. Mazilu, D. Ohlmann, M. Robino and G. Schwalbach, Applied Optics 37, No. 13 (1998) 2681.

[10] L. P. Colletti, J. Electrochem. Soc. 145 (1998) 1442.

[11] S. A. Ringel, R., Sudharsanan, A. Rohatgi, M. S. Owens and H. P. Gillis, Journal of Optoelectronics and Advanced Materials 7, No. 3, (2005) 1483. .

[12] K. Prasada Rao, O. Md Hussain, B. Srinivasulu Naidu and P. J. Reddy, Semicond. Sci. Technol. 12 (1997) 564.

[13] From ASTM x-ray powder data file, card No. 15-770.

[14] R. Kavitha and K. Sakthivel, Superlattices and Microstructures 86 (2015) 51.

[15] R. Swanepoel, J. Phys. E: Sci. Instrum. **17** (1984) 896.

[16] E. Márquez, E. R. Shaaban and A. M. Abousehly, Int. J. New. Hor. Phys 1 (2014) 17.

[17] P. Sharma and S. C. Katyal, J. Appl. Phys. 107 (2010) 113527

[18] T. S. Moss, Optical Properties of Semiconductors (London: Buttenvorths) (1959).

[19] M. Nowak, Thin Solid Films 266, 258 (1995).

[20] E. Márquez, J.M. González-Leal, A.M. Bernal-Oliva, R. Jiménez-Garay and T. Wagner, Journal of Non-Crystalline Solids **354** (2008) 503.

[21] E. R. Shaaban, I.S.Yahia, N.Afify, G.F.Salem and

© 2017 NSP
Natural Sciences Publishing Cor.

W.Dobrowolski, Materials ScienceinSemiconductorProcessing19, (2014) 107.

[22] E.A. Davis and N. F. Mott, Philos. Mag. **22** (1970), p. 903.

[23] M. Kastner, Physical. Review Letter 28, 355 (1972)

[24] E. A. Davis and N.F. Mott, Philos. Mag. **22** (1970), p. 903.

[25] J. Tauc, editor. Amorphous and liquid semiconductors. New York: Plenum Press; 1979. p. 159.

[26] E. R. Shaaban, I. S. Yahia, N. Afify, G. F. Salem and W. Dobrowolski, Materials Science in Semiconductor Processing 19 (2014) 107.

© 2017 NSP
Natural Sciences Publishing Cor.